IEEE Robotics and Automation Letters (RAL) paper presented at the
2020 IEEE/RSJ International Conference on Intelligent Robots and Systems (IROS)
October 25-29, 2020, Las Vegas, NV, USA (Virtual)

Kubits: solid-state self-reconfiguration with programmable magnets

Simon Hauser[1], Mehmet Mutlu[1], and Auke J. Ijspeert[1]

***Abstract*— Even though many prototypes of 3D self-reconfiguring modular robots (SRMRs) have been developed in recent years, a demonstration involving 1'000 modules remains a challenge. This is largely due to complex mechanics needed to achieve connection, disconnection and especially actuation in such a system. This work introduces "Kubits", which is, to the best of our knowledge, the first SRMR that achieves these functionalities without moving parts, i.e. in solid-state. Each module contains a kind of *programmable magnet* whose magnetization can be controlled. The simultaneous control of touching magnet pairs of two modules is used to create attraction (connection), neutrality (disconnection) and actuation (repulsion), which results in self-reconfiguration by a cube pivoting around an edge. We detail the design of the system and demonstrate a series of successful flips, including a jumping mode. The energy-efficient, lightweight and robust (both in terms of mechanics and control) method in Kubits is a promising path for scalable self-reconfiguration.**

I. INTRODUCTION

Self-reconfigurable modular robots (SRMR) are a unique subsection of robot types in modular robotics, where robots are built out of modules that can self-reconfigure. The development of SRMR systems is motivated by three features, formulated in [1]: (i) *versatility and adaptability*, meaning that the system is capable to adapt its morphology to one that is better suited for an (unknown) set of tasks, (ii) *cheap compared with their complexity*, meaning that complex systems can be constructed out of cheap mass-produced simple modules, and (iii) *robust*, meaning that a full system failure can be solved by replacing malfunctioning single modules.

All the SRMR systems developed over the last 30 years aimed at demonstrating the features described above. However, there is an ongoing debate if the research on SRMR system has delivered on any of them: modules of developed systems are often fragile, it can be difficult to assign different tasks to a compound of modules, and the prototype stage of such research makes modules expensive to produce. This is why many SRMR systems - especially in 3D - were only shown as a proof of concept, usually with a limited number of functional modules ($<$10 and up to dozens). To bring the research in SRMR one step forward, the demonstration of a system with at least 1'000 modules is denoted as a "Grand Challenge" in [2]. They note that in order to achieve this, 'rethinking of key hardware issues' is required.

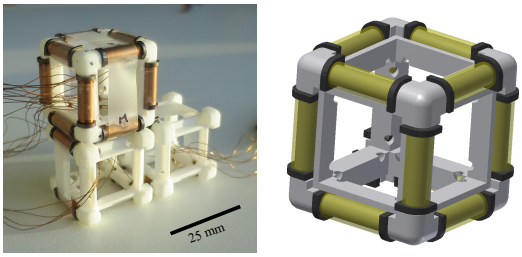

Fig. 1. Left: The Kubits self-reconfiguring modular robot system with one fully and two partially equipped modules. Right: Schematic of a single Kubits module with flat poles PRMs.

In this work, we introduce "Kubits", a novel SRMR system with a radically different hardware solution based entirely on magnets (Fig. 1) which are used for connection, disconnection and actuation. Even though magnets were used in many of the previously developed systems, they were mostly used to either take over or assist the connection functionality. Permanent magnets can be interesting due to both their powerless holding characteristic and self-alignment properties when implemented appropriately. However, disconnecting permanent magnets ironically requires a dedicated mechanism which can add significant complexity. If permanent magnets are only used for self-aligning purposes such as e.g. in Roombots [3], the weight of the robot can be used to break the attraction. Other systems use permanent magnets as their primary connection method, and previous solutions for disconnection include shape memory alloys (SMA) in [4], and a flywheel in [5, 6] which at the same time is used as the actuation method. Electromagnets (EM) can display similar characteristics as permanent magnets with the advantage of being controllable, however the powerless holding property is lost. The disadvantages of power draining electronics to keep up the magnetic field of an EM and resistive heat generated thereby makes this kind of magnets unfeasible to be used in SRMRs. Alternatively, a different kind of magnet called "electropermanent magnet" (EPM) recently has been developed [7]. It essentially represents a permanent magnet that can be "switched on" and "switched off" by short electric pulses, eliminating the disadvantages of EMs while keeping the main advantages of permanent magnets. These magnets have successfully been integrated in a number of SRMRs for both the connection and disconnection functionalities (e.g. in [8, 9]). Nevertheless, a separate actuation method still is required, again adding complexity.

This project is funded by the Swiss National Science Foundation (Project 200021_153299) and the Fundação para a Ciência e Tecnologia (FCT) agency of Ministry for Education and Science of Portugal (PD/BD/105781/2014).

[1]Simon Hauser, Mehmet Mutlu and Auke Ijspeert are with the Biorobotics Laboratory (BioRob), School of Engineering, Institute of Bioengineering, Ecole polytechnique férérale de Lausanne (EPFL), Switzerland, simon.hauser@alumni.epfl.ch

To circumvent the frequent issues of mechanically fragile and complex methods to achieve all three functionalities connection, disconnection and actuation, Kubits is the first solid-state module that can fulfil these functionalities with no moving parts within a module. Inspired by the work on EPMs, we developed a "programmable magnet" (PRM) whose magnetization can be controlled to three states ("+" polarization, "-" polarization and neutral state). Each of the three states is stable, meaning no power is needed to keep an PRM in such a stable state, and each of these states fulfills a functionality in the Kubits SRMR system: attraction (connection), neutrality (disconnection) and actuation (repulsion), which results in self-reconfiguration by a cube pivoting around an edge. Switching the states for the different functionalities is achieved by short electric pulses, making the self-reconfiguration energy efficient. Moreover, because the module is solid-state, the complexity of a module in comparison to contemporary SRMRs is dramatically reduced, making it less fragile, reducing costs due to simplified mechanics, and reducing weight. These aspects could pave the way for such a system to display scalability to tens of modules, potentially reaching the proposed challenge of 1'000 modules.

Other than being a novel SRMR research platform, we envision Kubits to be used as an educational tool or a high-tech toy. In general, a user could create a variety of structures. Works like [10] already offer a potential way to create meaningful objects/structures for a given task using voxel shaped modules such as Kubits. Further, the size of Kubits currently is limited due to the developed actuation method, however it is also applicable in microgravity environment where constraints due to gravity can be relaxed to allow bigger modules. A more futuristic application thus could be in space, where Kubits could be smart transportation boxes or intelligent building bricks to assemble large structures while being carried to space in a compact volume of rocket payload fairing. The closest work in the space-related literature appears in [11], where pivoting cubes are described that use conventional electromagnets (EMs) to perform attraction and repulsion actions, and in [12], the 6 DoF formation flight in microgravity environment and wireless power transfer between modules is demonstrated, hinting at the potential SRMRs could have in space applications.

II. MATERIALS AND METHODS

A. Overall concept

The proposed mechanism is based on magnetic attraction and repulsion forces. Copper wire is wrapped around a soft magnet (Alnico 500), creating a coil. Sending electrical pulses with high current through the coil influences the polarization of the magnet (Fig. 2). A strong enough pulse can bring the magnet to its polarized state (in either direction, further denoted "+" and "-"). Additionally, a weaker pulse from either side of the polarization can bring the magnet to its coercivity at which the magnetic flux of the magnet disappears (further denoted as "0"). These three states can produce states of attraction, repulsion or neutrality between two adjacent magnets. The arrangement of a multitude of such programmable magnets (PRM) in Kubits is such that the state of attraction is used as the functionality connection, neutrality is used as disconnection, and repulsion is used as actuation. The following sections first describe the parameters of a 3-state PRM and then how these states are used to design the SRMR Kubits.

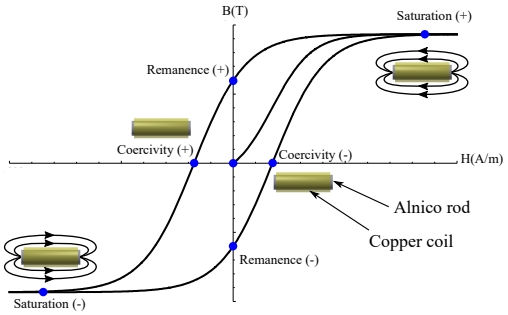

Fig. 2. A typical flux density (B) vs magnetizing force (H) plot for soft magnets exhibiting hysteresis effect.

B. Design of the 3-state PRM

A related class of magnets - which possesses two stable states through the same polarization method - are the so-called electropermanent magnets (EPM). In the research in [7], it is described that due to scaling properties of the switching energy in relation to the holding force, EPMs are more interesting for small scale applications. This is likewise the case for PRMs, and thus our aim was to obtain a small and powerful magnet.

We started with the magnet as the core component around which the system is built and chose commercially available Alnico rods of 3 mm diameter ($= d_{mag}$) and 12 mm length ($= l_{mag}$) with a remanence of 1.1 T ($= Br_A$). We defined a copper coil which can create a strong enough magnetic field to polarize the magnet. To use off-the-shelf electronic components, the supply voltage is chosen as 24 V ($= V_{max}$) and the current requirement per magnet to be below 15 A.

We developed a small graphical user interface (GUI) based on the formulas in [7] that quickly let's us change the design parameters, outputting the corresponding control parameters. As a starting point, we used the current needed to magnetize the Alnico rod, assuming that the rod is in contact with iron, i.e. the gap g between rod and iron is $g = g0 = 0$ m for all calculations. In this case, the current is given by

$$I_{max\_g0} = \frac{H_{ext} \cdot l_{mag}}{N}, \tag{1}$$

where H_{ext} in [A/m] is the external magnetizing force required to reach magnetic saturation of Alnico and N is the number of turns of the coil. As a rule of thumb, H_{ext} should be at least 3 times the coercive force $H_{c\_A} = 50'400$ A/m of the used Alnico rod, i.e. $H_{ext} = 3 \cdot H_{c\_A} = 151'200$ A/m. From Eq. 1, a coil with at least 120 turns is needed to keep I_{max_g0} below 15 A, and a current of 10 A would require 180 turns.

We used these requirements to define the coil parameters. To minimize the final weight and size of the coil, a single-layer coil with thin wire would be optimal. However, thin wire has a higher resistance which depends on the cross-sectional area of the wire, such that the supply voltage of 24 V could not achieve a current pulse of roughly 10 A - 15 A if the resistance of the coil is higher than 2 Ohm. A multi-layer coil thus was needed, where the combination of wire diameter and number of turns should result in an integer number of layers. Testing a variety of combinations with the GUI, we chose a copper wire with a diameter of $d_{wire} = 0.15$ mm, resulting in a 3-layer coil with $N = 168$ turns, and thus $I_{max\_g0} = 10.8$ A.

Next, we calculated the theoretical coil resistance. The following series of equations were used:

$$A_{wire} = \frac{\pi}{4} \cdot d_{wire}^2 \tag{2}$$

$$w_{coil} = \frac{N \cdot d_{wire}^2}{l_{mag}} \tag{3}$$

$$l_{wire} = N \cdot \pi(d_{mag} + w_{coil}) \tag{4}$$

$$R_{wire} = \frac{l_{wire}}{A_{wire}} \cdot r_{copper}. \tag{5}$$

In Eq. 2, A_{wire} in [m^2] is the cross-sectional area of the wire. Eq. 3 is used to calculate the width of the coil w_{coil} in [m], assuming square wire packing. In Eq. 4, the length of the wire l_{wire} in [m] is calculated by summing up N times the length of an averaged middle turn. Finally, Eq. 5, the wire resistance R_{wire} in [Ω] is given by multiplying the ratio of l_{wire} and A_{wire} with the specific resistance of copper $r_{copper} = 1.68e^{-8}$ Ωm. The theoretical coil resistance is $R_{wire} = 1.6633$ Ω.

The minimal voltage supply V_{min} at $g0$ can now be calculated as $V_{min\_g0} = R_{wire} \cdot I_{max\_g0} = 17.964$ V. As the final variable, the coil inductance L_{coil} in [H] is needed, which is calculated as

$$L_{coil} = \frac{N^2 \cdot \pi \cdot d_{mag}^2 \cdot N_{rods}(B_{sat\_A} + Br_A + \mu_0 \cdot H_{sat\_A})}{8 \cdot H_{sat\_A} \cdot l_{mag}}. \tag{6}$$

In Eq. 6, $N_{rod} = 1$ is the number of magnet rods in the system, $B_{sat\_A} = 1.42$ T is the saturation magnetic flux of the used Alnico material, and $\mu_0 = 1.257e^{-6}$ H/m is the vacuum permeability, resulting in $L_{coil} = 1.4899e^{-4}$ H.

Lastly, the pulse length to magnetize the Alnico rod can be obtained with

$$T_{sat} = \frac{L_{coil}}{R_{wire}} \cdot \log\left(\frac{V_{max}}{V_{max} - V_{min\_g0}}\right), \tag{7}$$

resulting in $T_{sat} = 1.2364e^{-4}$ s, or around 124 μs. Bringing the magnetization to the coercivity where the magnetic flux disappears will require a shorter pulse, however we could not find a systematic way of obtaining this pulse length and thus will find it experimentally, as described in section III.

C. Magnetic hinge with PRMs

To direct the magnetic flux at the end of the rod to the specific locations, iron poles are glued onto each side of the rod. The material of these poles should be chosen to minimally disturb the flux of the magnet, and thus we used 1 mm thick ARMCO iron with a maximal flux density of 2.075 T ($= B_{sat\_I}$). The poles additionally serve the purpose to create a magnetic hinge between a PRM pair. This hinge enables modules to perform self-reconfiguration by acting as dynamic links between modules. We designed and tested two different versions of the poles to create the hinge. The first design consists of two flat regions connected over a 90 deg circular arc (Fig. 3 (a1)). The length of the flat region defines the contact area between a PRM pair, which can be optimized (i.e. reduced) until the iron saturation is reached, i.e.

$$b_{contact} = \frac{Br_A}{B_{sat\_I}} \cdot \frac{\pi \cdot d_{mag}^2 \cdot N_{rods}}{4a_{contact}}, \tag{8}$$

and with $a_{contact} = 1$ mm, $b_{contact}$ equals 3.7 mm. The second pole design consists of a fully circular shape without the flat regions (Fig. 3 (c1)), allowing a PRM pair to rotate more freely. A PRM pair uses the arc section of the poles to rotate around each other. Concerning the holding force of magnets, with the values of $a_{contact}$ and $b_{contact}$, a theoretical force of $F_{max} = B_{sat\_I}^2 \cdot a_{contact} \cdot b_{contact}/\mu_0 = 12.8354$ N can be calculated. For the preliminary experiments presented in this work however, this force has not been considered or verified. This is in part because during the pivot, the contact area between PRM pairs is reduced to a contact line for which we did not calculate a theoretical holding force. Moreover, in the case of the circular poles, PRM pairs are always only in line contact with each other, potentially displaying reduced holding force characteristics. Detailed holding force measurements is work of future research.

Fig. 3 shows the schematics of the two designs of 3-state PRMs, the manufactured PRMs and their behavior as the hinge mechanism of PRM pairs to enable the pivoting motion. The physical parameters of the components are given in Tab. I. A total of 24 PRMs have been produced, 12 of each version.

D. Design of the cubic module

For the design of the module, we took inspiration from the *pivoting cube model*, described in [2] and used in M-Blocks [5, 6], where cubes in a lattice self-reconfigure by pivoting around one of their edges. Each Kubit is a cube where each edge is equipped with a PRM, resulting in 12 PRMs per module, and thus each PRM is shared between two different faces of the cube (see Fig. 1). When the faces of two modules meet in an aligned manner, there will always be four PRMs of the face of one cube coming into contact with four PRMs of the face of the second cube, forming in total four PRM pairs. The PRMs now work in three different modes to achieve the main functionalities: (i) For forming a connection between two module faces, the polarization of each PRM pair is such that they attract each other, that is the "+" pole of each PRM in the pair is in contact with the "-" pole of the respective other PRM; (ii) For disconnecting two module faces, each PRM is put into its neutral state at its coercivity at which no attraction forces between PRM pairs

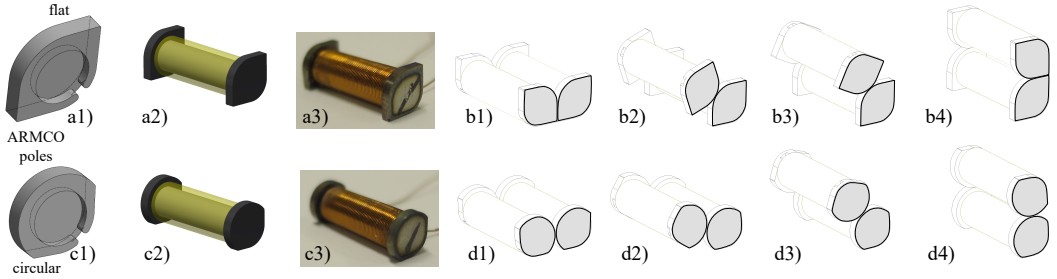

Fig. 3. The two PRM designs and their behavior as magnetic hinges. (a1) CAD design of the flat pole, (a2) schematic and (a3) manufactured flat pole PRM design. (b1-b4) Pivoting hinge behavior of the flat pole PRM pair. (c1) CAD design of the circular pole, (c2) schematic and (c3) manufactured circular pole PRM design. (d1-d4) Pivoting hinge behavior of the circular pole PRM pair.

exist and the faces separate under no load; (iii) For actuation, the polarization of at least one PRM pair is such that they repulse each other, that is the "+" pole of one PRM in the pair is in contact with the "+" pole of the other PRM and analog for the "-" pole. This makes the PRMs of this pair separate from each other due to magnetic repulsion forces. This motion is converted into a rotation around the edge of a module by using another PRM pair as the magnetic hinge described above, resulting in a pivot. A combination of these modes allow every cube present in the lattice to pivot around any of its edges as long as no collisions occur, and thereby achieve self-reconfiguration. Fig. 4 shows the first basic example of a traverse flip. Two modules form the base and a pivoting module is attached on top of one base module. The PRM pairs are pre-configured to attraction and neutral states prior to attachment. After attachment, one PRM pair between a base and pivoting module is set to repulsion, upon which a rotation around the opposite magnetic hinge is initiated. The pivoting module reattaches to the second base module after completing a 90 degree rotation.

Given the dimensions of the PRM, a cubic lattice with a unit voxel of 25 mm for each side length was chosen. SLS printing was used to manufacture 4 cube skeletons with side length of 24 mm. The PRMs are glued into the edges, protruding the skeleton 0.5 mm on each side, ensuring a clean contact between PRM pairs. All the electronics was kept outside. Integrated electronics for autonomous modules is work of future research.

TABLE I

WEIGHTS OF MECHANICAL COMPONENTS.

cylindrical Alnico 500 rod (h=12mm, d=3mm)	≈650 mg
copper coil (wire d=0.15, 168 turns)	≈380 mg
pair of flat poles (ARMCO iron, h=1mm)	≈220 mg
assembled PRM	≈1260 mg
cubic skeleton (SLS printing)	≈1850 mg
Kubit with 3 PRMs	≈5.5 g
Kubit with 12 PRMs	≈17 g

E. Electronics

At the moment, each PRM is controlled by an own H-bridge for a more flexible setup during the experimental phase. The driver that fulfills the necessary specifications is VNH7040AY. When multiple PRMs are triggered at the same time, the current demand rises drastically. We also use a large capacitor (22 mF, 35 V) in parallel to the power supply to prevent rapid supply voltage drop. The switching is controlled by an Arduino Nano. For the preliminary experiments, we only developed the electronics to control up to two PRM pairs at the same time.

III. EXPERIMENTS

A. Verification of the manufactured PRM

The resistance of the coil in the manufactured PRMs is measured at roughly $R_{wire} = 2\ \Omega$, higher than the calculated 1.6633 Ω. This is likely due to additional wire needed for forming contacts as well as a less optimal packing factor which results in a longer wire, increasing the resistance. This affects V_{min_g0}, which now becomes 21.6 V, in turn modifying the theoretical pulse length according to Eq. 7 to $T_{sat} = 185\ \mu$s.

B. Remanence saturation pulse length

These experiments aimed at validating that the developed electronics are able to fully magnetize the PRM, and finding the actual pulse length for magnetizing the manufactured PRM according to the modifications outlined above. Depending on the length of the pulse, the magnet gets magnetized weaker or stronger. We magnetized an isolated PRM in air after electrical pulses of different lengths and used a gaussmeter to measure the open circuit magnetic flux. It is important to note that this measurement is considerably lower than the remanence at 1.1 T (closed circuit magnetic flux) and depends on the shape of the magnet, however it exhibits the same saturation characteristic. The results are summarized in Tab. II. For each tested pulse length, the obtained magnetic strength is indicated with the standard deviation of the 5 trials.

TABLE II

MAGNETIC STRENGTH OF MAGNETIZING DEPENDING ON PULSE LENGTH T_{sat}. SUPPLY VOLTAGE IS 24 V.

pulse length [μs]	100	125	135	145	165	900
strength $\pm$1 [mT]	118	122	123	124	125	125

It can be seen that the calculated pulse length of 185 μs approximately corresponds with the measured saturation

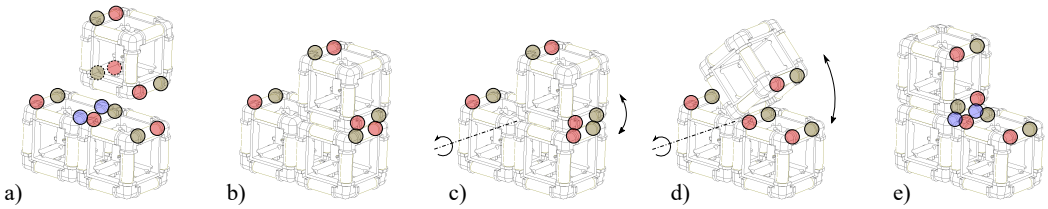

Fig. 4. Basic traverse flip. (a) PRM pairs are preconfigured into attraction and neutral states. (b) The pivoting module attaches to one of the base modules. (c) One PRM pair between a base and pivoting module is set to repulsion, initiating a rotation around the opposite magnetic hinge. (d) Rotation around the magnetic hinge. (e) The pivoting module reattaches to the second base module. Red circle: "+" pole of a PRM, green circle: "-" pole of a PRM, blue circle: "0" neutral pole of a PRM.

pulse length of 165 μs. Further, the saturation characteristic is such that a somewhat too-short pulse (e.g. 125 μs) does not drop the strength substantially.

C. Coercivity pulse length

To achieve the neutral state of the PRM, the Alnico rod has to be brought to its coercivity, at which the magnetic flux disappears. By using the same voltage source, this can be achieved by sending a shorter pulse through the coil. We first fully magnetize the PRM in air. We then send a shorter pulse $T_{coercivity} < T_{sat}$ in opposite polarization direction through the coil and reassess the magnetic strength with the gaussmeter where the goal was to reach 0 T. At 24 V, we experimentally found that this is achieved by a pulse length of 39 μs, resulting in almost perfect demagnetization ± 1 mT. Although manufacturing variances influence these pulse lengths, at the current stage we used the indicated values for all PRMs; in-depth research could tailor the values to each PRM through individual calibration.

D. Pivoting with a partially equipped module

This set of experiments were done with PRMs mounted in the actual module skeletons. In these experiments, the electronics were limited to simultaneously control only two PRMs at a time, such that the properties of one PRM pair is controlled. The setup of the pivoting experiments involves three modules: two modules form the base and one module performs the pivot. Each module is only equipped with the PRMs necessary for this pivot, i.e. three PRMs in each module. This is especially important for the pivoting module which in this configuration is as light as possible. To test if the movement created by the repulsion of one PRM pair is enough to achieve flipping, we initially created reduced weight conditions (each module weights around 5.5 g).

Before the pivot, all the involved PRM pairs are first configured such that the pivoting module attaches to one of the base modules, as well as ensuring that the PRM pairs configuration for after the pivot is such that the pivoting module can attach to the second base module (see Fig. 4 for reference). From the initial configuration, the PRM pair opposite the PRM pair functioning as the magnetic hinge is set to repulsion, upon which the pivoting cube performs the rotation around the hinge, detaching from the first base module and reattaching to the second base module.

This basic pivot is performed in various configurations, e.g. as a traverse flip, upside-down traverse flip, sideways flip, up-to-down flip and down-to-up flip. We also included the scenario where the pivoting module performs a 180 degrees upwards flip, the most difficult case. We tested each configuration for the successful execution of the flip first with the flat pole design, and then repeated them with the circular pole design. Each experiment was filmed once in real time at 60 fps and once with a high-speed camera at 960 fps.

E. Back-and-forth pivoting with a partially equipped module

In this experiment, the pivoting module continuously flips back and forth between the two base modules. We did not realign the pivoting module after each flip, but rather wanted to validate if the alignment property of the magnet themselves is enough to make the pivoting module attach in a position suitable for a subsequent flip.

F. Pivoting with a fully equipped module

A subset of the flips, including the traverse flip and the down-to-up flip, was repeated with the pivoting module equipped with all 12 PRMs. This increased the weight of this module from 5.5 g to 17 g, which made the flipping substantially more challenging.

G. Jumping with a partially and fully equipped module

Additionally, we performed jumping experiments involving two modules and to PRM pairs controlled at the same time. The jumping module is attached to the base module with two PRM pairs. Then, both PRM pairs are switched to repulsion at the same time, causing the jumping module to be launched vertically into the air. We performed the experiment both with a partially and fully equipped jumping module.

IV. RESULTS AND DISCUSSION

A. Pivoting with a partially equipped module

Our first attempts of performing the traverse flip with the pulse lengths selected above were unsuccessful. The observation was that a repulsive motion between the PRM pair in question seemed to occur, however the PRM pair would immediately go back to attraction, reattaching the flipping cube to its original base module. The reason for this behavior was found in the low coercive force of Alnico that allows the simple manipulation of the magnetic field to begin with: because the magnetic field of Alnico can easily

be controlled by an external field, it is in turn also susceptible to external field disturbances that can cause demagnetization. In our case, this meant that even though we magnetize the PRM pair to achieve repulsion by applying the required pulse to both PRMs, immediately after the pulse the magnetic fields of both PRMs would start to interfere with each other, resulting in demagnetization. This happens in a very short time frame, effectively cancelling the repulsive motion.

Our hypothesis was that this issue could be solved by applying a longer pulse $T_{repulsion} > T_{sat}$, which would have two effects. On the one hand, the magnetic field created by the coil can help to stabilize the magnetic field of the Alnico such that it is less influenced by external demagnetizing fields. On the other hand, the magnetic field created by the coil itself can act as an electromagnet for as long as the pulse is active, and thus the repulsion is assisted by the two electromagnetic components of the PRM pair.

We tested our hypothesis by gradually increasing the pulse length for repulsion $T_{repulsion}$ and observing the flipping behavior. We experimentally found that a flipping motion could be achieved with $T_{repulsion} = 100$ ms. Note that this is over 600 times longer than $T_{sat} = 165$ μs. The longer pulse duration on the one hand requires substantially more energy per flip, which will be an important factor to consider for a mobile power supply once a fully autonomous system is developed. On the other hand, temperature increase in the PRM due to resistive heating can be observed, possibly hindering the continuous operation of flipping motions. Additionally, it has to be investigated if the field of the repulsing PRM pair is affecting the strength of the other PRMs present in the system, even though we did not observe this in the present set of experiments. These considerations are out of scope in the current stage of the project but need to be taken into account for future research.

The traverse flip is shown in Fig. 5 (a-d), and the flipping behavior of all experiments can be seen in the supplementary video. It is important to note that the hinge PRMs with circular poles resulted in a smoother flipping motion. In fact, only the circular poles were able to achieve the 180 degrees upwards flip. The reason for this is the attraction force in the contact areas of the flat poles. Consider a PRM pair with flat poles as the magnetic hinge around which the pivoting module rotates. Once the repulsion movement created by the opposing PRM starts, the momentum generated by it first needs to separate the attracting regions of the hinge PRM before the arc section allows the rotation. This separation instantaneously manifests as a normal force between attracting regions, which is the preferred direction of magnetic attraction, and thus a part of the generated momentum is lost to achieve this separation. In contrast, the circular poles do not suffer from this phenomenon. The entire momentum generated by the repulsion can immediately be converted into the rotation around the hinge, allowing the pivoting module to preserve the extra energy to complete the 180 degrees upwards flip. As mentioned earlier, the trade-off for the circular poles may be a reduced attraction force due to a reduction of the optimal contact area to a contact line.

B. Flipping energy and torque

Assuming a constant current and a constant voltage during a pulse, we can calculate the energy needed for a flip by simply putting $E = V \cdot I \cdot \Delta t = V_{max} \cdot \frac{V_{max}}{R_{wire}} \cdot \Delta t = 24 \cdot \frac{24}{2} \cdot \Delta t$ Ws (or J). In our current setup (Fig. 4), a flip involves the correct magnetization of 6 PMRs, neutralization of 1 PRM, and then repulsion of one PRM pair. This results in $E_{flip} = 6 \cdot E_{sat} + 1 \cdot E_{coercivity} + 2 \cdot E_{repulsion} = 6 \cdot 13.2\mu Wh + 3.1\mu Wh + 2 \cdot 8mWh \approx 16.1$ mWh or ≈ 57.9 J.

We estimated the torque created by one repulsing PRM pair through deriving the equation of motion for a simplified model of a pivoting module. The repulsing torque M induces a rotation with angle θ around a fixed point, which is counteracted by the mass m of the module at distance L and the inertia I. The equation of motion is then given by $(mL^2 + I)\ddot{\theta} = M - mgL\cos(\theta + \pi/4)$. We extracted the rotation angle during the traverse flip for both the partially and fully equipped case from the high-speed recordings, and approximated both movements with a sine function to compute an analytical angular acceleration. By substituting the corresponding parameters (extracted from the CAD model, i.e. $L_{3PRMs} = 10.28$ mm, $L_{12PRMs} = 12.5$ mm, $I_{3PRMs} = 2148$ g mm^2, $I_{12PRMs} = 7720$ g mm^2, and m_{3PRMs} and m_{12PRMs} taken from Tab. I), we can solve for M for both cases. Fig. 6 shows the torque estimations from one repulsing PRM pair for $0 \leq \theta \leq \pi/4$ for both flips together with the used model. Although our model likely does not capture the full dynamics of the repulsive moment, both cases indicate a similar initial torque peak of roughly 10 mNm, rapidly declining with an increasing rotation angle.

C. Back-and-forth pivoting with a partially equipped module

The supplementary video shows continuous back-and-forth pivoting of a traverse flip. In total, 8 uninterrupted subsequent flips were successfully executed. Misalignments after each flip occur due to slipping effects in the PRM acting as the hinge: the impact momentum generated by the repulsing PRMs causes the pivoting module to rotate faster around the stationary part of the hinge such that the intended actual joint rotation starts with a slight delay. Such slipping effects could be suppressed in future versions by including mechanical features in the pole design (such as e.g. gear-toothed poles, similar to [6]). Even though relatively large misalignments can be observed (Fig. 5e), the method was able to handle such cases, showcasing interesting robustness properties. The experiment was stopped after 8 flips due to the heating of the involved PRMs. Heating thus is a limitation in the current system, however the frequency and complexity of a self-reconfiguration strongly depends on the actual application (e.g. a continuously running fast reconfiguration vs. an slow, iterative reconfiguration).

D. Pivoting with a fully equipped module

As can be seen in the video and in Fig. 5, we successfully could demonstrate a traverse flip with a fully equipped module. We also show an unsuccessful attempt of performing a down-to-up flip where the generated momentum is clearly

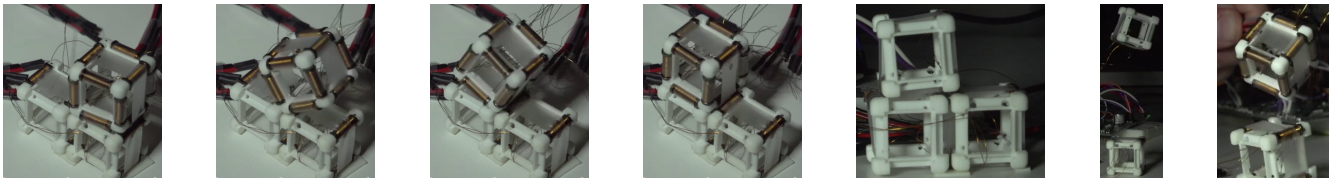

(a) t=16.6ms (b) t=50ms (c) t=83.3ms (d) t=116.6ms (e) misalignments (f) (g)

Fig. 5. (a-d) Snapshots of a fully equipped Kubits module performing the traverse flip. (e) Accumulated misalignment after 7 back and forth flips. (f) Captured apexes of jumping using two PRM pairs repulsing simultaneously of a partially and (g) fully equipped module.

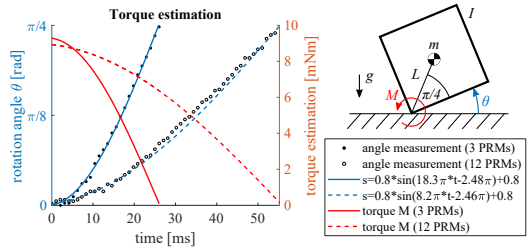

Fig. 6. Torque estimation of a repulsing PRM pair in both partially and fully equipped module and model used to derive the equation of motion of the pivoting cube. A peak torque of around 10 mNm is observed in both cases, rapidly declining with an increasing rotation angle.

not enough to pivot against gravity. However, it is important to keep in mind that the rotation momentum at the moment is created by the repulsion mode of one PRM pair only. Besides the PRM pair that is used as the hinge, there are two additional PRM pairs that at the moment stay in their neutral states for the entire duration of the experiments. We did not develop the necessary electronics to control four PRM pairs at the same time, however these two PRM pairs can readily be used to assist the momentum creation likewise through their repulsion mode. With considerations on the actual polarizations in the adjacent PRM pairs and effects such as mutual inductance, it will be work of future research to investigate if this could substantially boost the pivoting performance.

E. Jumping with a partially and fully equipped module

The jumping behavior shows an interesting mode for separating modules. Even though it is unlikely that this mode can be used for self-reconfiguration, launching modules could provide e.g. an emergency mode of rapid disconnection or module repositioning. It is unclear at the moment how precisely the launching velocity and trajectory could be controlled to properly assess the usefulness of jumping. Nevertheless, both the partially and fully equipped module could successfully get launched. The lighter module achieved a jumping height of approximately 10 cm before the wires of the PRMs stopped the motion (Fig. 5f). The heavier module achieved a jumping height of approximately 3 cm (Fig. 5g). Jumping will need to be revalidated in untethered scenarios with autonomous modules.

F. Key features of the Kubits design

Kubits have several key aspects that can make it viable to be used in a large number of modules. The switch between states of the proposed 3-state PRM is achieved by a short electric pulse which makes it energy efficient and fast. Additionally, each of the 3 states is stable, meaning no power is needed to keep an PRM in such a stable state. A connected structure held together by attractive magnetic forces will thus keep its shape powerless, and can be transferred into a neutral bulk of modules that also do not require any energy for keeping their neutral state after the transition. The module is solid-state, meaning there are no moving mechanical parts required for any of the functionalities. This makes them mechanically more robust and cheaper to produce and assemble. The reduced mechanical complexity makes the modules lighter which is crucial for scalability, i.e. a system of 1'000 modules is only realizable with strong but lightweight modules, thus weight reduction has a major importance. Besides continuously powering a microcontroller in a fully autonomous version, each module consumes only power for switching PRMs, enabling efficient power distribution strategies (e.g. potentially only one or a few modules contain batteries and power all attached modules through electrical contacts when connected).

V. CONCLUSION AND FUTURE WORK

In this work, we introduced a self-reconfigurable modular robot (SRMR) system "Kubits", the first solid-state system that can perform self-reconfiguration without moving parts. The simple, lightweight mechanical design and energy efficiency of Kubits brings several advantages over other contemporary designs, where fragile, heavy and expensive (both cost- and energy-wise) mechanics for self-reconfiguration is often the bottleneck in scaling the design into thousands of modules.

The Kubits system is based on magnetic forces. Inspired by previous work on controllable magnets, we developed a "programmable magnet" (PRM) based on a soft Alnico rod whose polarization can be controlled by short electric pulses through a coil wrapped around the rod. The PRM has three stable magnetization states: the "+" polarization, the "-" polarization, and the neutral state at coercivity where the magnetic flux disappears. A pair of PRMs can use these states to realize the three main functionalities of an SRMR: an attracting magnetization is used as connection, a neutral magnetization is used as disconnection, and a repulsing

magnetization is used as actuation. We then designed a cubic module where each edge of the cube contains a PRM. When two faces of two modules meet, they create four PRM pairs. By appropriately choosing the magnetization of these four pairs, one pair is used to create a magnetic hinge through attraction whereas the opposing pair is used to create an impulse momentum through repulsion. This causes the module to pivot around the formed hinge, thereby achieving self-reconfiguration. In such a system, each cube is able to pivot around any of its edges, forming a lattice-type SRMR system.

In the preliminary experiments presented in this work, we first detail the development of the PRM based on equations of a similar type of magnets, and verify the theoretical control parameters experimentally. We then introduce the design of the cubic module into which we integrated two different versions of PRMs. We successfully demonstrate a variety of pivoting scenarios with our proposed system, including traverse flip, upside-down traverse flip, sideways flip, up-to-down flip, down-to-up flip, and a more difficult upwards flip. We derived a simple model to estimate the torque generated by a repulsing PRM pair, showing that the flips are achieved by a torque in the order of 10 mNm. Additionally, with two repulsing PRM pairs, we perform a jumping scenario where a module gets launched into the air. Based on the successful performance of the produced prototypes, we see Kubits as a promising new SRMR system. The mechanical simplicity of Kubits together with the fast and energy efficient method to create connection, disconnection and actuation could pave the way towards a 3D SRMR system with 1'000 or more modules.

As future work, there are many possible ways to progress. The mechanical design of Kubits is in a prototype stage and could be improved towards reducing misalignment issues. The design of the poles could be optimized towards striking a balance between strongest attraction forces (flat pole design) and least momentum loss (circular pole design). Additionally, for a better understanding of the transient force responses between a PRM pair during polarization periods, especially during repulsion, a full 3D magnetic simulation of the device would likely provide valuable insight. This would also indicate the limitations of the method, which currently seems only applicable to small-scale modules. This is due to the scaling factor between the created (electro)magnetic force and the weight of a PRM, i.e. larger modules are likely to be too heavy to use the same technology for self-reconfiguration. With the goal of developing a fully autonomous and untethered system, the biggest challenge thus is developing and downsizing the electronics to fit inside Kubits, achieving a self-contained module with own power, computation and wireless communication capabilities that can do all of the tasks presented in this paper.

References

[1] Kasper Stoy, David Brandt, and David J. Christensen. *Self-reconfigurable robots: an introduction*. Intelligent robotics and autonomous agents. Cambridge, Mass: MIT Press, 2010.

[2] M. Yim, Wei-Min Shen, B. Salemi, D. Rus, M. Moll, H. Lipson, E. Klavins, and G.S. Chirikjian. "Modular Self-Reconfigurable Robot Systems [Grand Challenges of Robotics]". In: *IEEE Robotics Automation Magazine* 14.1 (Mar. 2007), pp. 43–52.

[3] S. Hauser, M. Mutlu, P. -A. Léziart, H. Khodr, A. Bernardino, and A. J. Ijspeert. "Roombots extended: Challenges in the next generation of self-reconfigurable modular robots and their application in adaptive and assistive furniture". en. In: *Robotics and Autonomous Systems* (Feb. 2020), p. 103467.

[4] S. Murata, E. Yoshida, A. Kamimura, H. Kurokawa, K. Tomita, and S. Kokaji. "M-TRAN: self-reconfigurable modular robotic system". en. In: *IEEE/ASME Transactions on Mechatronics* 7.4 (Dec. 2002), pp. 431–441.

[5] J. W. Romanishin, K. Gilpin, and D. Rus. "M-blocks: Momentum-driven, magnetic modular robots". In: *2013 IEEE/RSJ International Conference on Intelligent Robots and Systems*. Nov. 2013, pp. 4288–4295.

[6] John W. Romanishin, Kyle Gilpin, Sebastian Claici, and Daniela Rus. "3D M-Blocks: Self-Reconfiguring robots capable of locomotion via pivoting in three dimensions". In: *International Conference on Robotics and Automation (ICRA)*. IEEE, 2015, pp. 1925–1932.

[7] Ara N. (Ara Nerses) Knaian. "Electropermanent magnetic connectors and actuators : devices and their application in programmable matter". eng. Thesis. Massachusetts Institute of Technology, 2010.

[8] Tarik Tosun, Jay Davey, Chao Liu, and Mark Yim. "Design and characterization of the EP-Face connector". In: *Intelligent Robots and Systems (IROS), 2016 IEEE/RSJ International Conference on*. IEEE, 2016, pp. 45–51.

[9] Bahar Haghighat, Emmanuel Droz, and Alcherio Martinoli. "Lily: A miniature floating robotic platform for programmable stochastic self-assembly". In: *Robotics and Automation (ICRA), 2015 IEEE International Conference on*. IEEE, 2015, pp. 1941–1948.

[10] Mihai Andries, Atabak Dehban, and José Santos-Victor. "Automatic Generation of Object Shapes With Desired Affordances Using Voxelgrid Representation". In: *Frontiers in Neurorobotics* 14 (2020), p. 22.

[11] M. Nisser, D. Izzo, and A. Borggraefe. "An Electromagnetically Actuated, Self-Reconfigurable Space Structure". en. In: *Transactions of the Japan Society for aeronautical and space sciences* 14 (2017), pp. 1–9.

[12] Allison K. Porter, Dustin J. Alinger, Raymond J. Sedwick, John Merk, Roedolph A. Opperman, Alexander Buck, Gregory Eslinger, Peter Fisher, David W. Miller, and Elisenda Bou. "Demonstration of Electromagnetic Formation Flight and Wireless Power Transfer". In: *Journal of Spacecraft and Rockets* 51.6 (2014), pp. 1914–1923.